S. LIPA*#, J. SAWICKI*, K. DYBOWSKI*, R. PIETRASIK*, B. JANUSZEWICZ*

THE EFFECT OF NON-METALLIC INCLUSIONS FORMED AS A RESULT OF DEOXIDATION ON THE FATIGUE STRENGTH OF 15CrNi6 AND 16MnCr5 STEEL

This paper presents the findings of fatigue strength tests of 15CrNi6 steel following low-pressure carburizing and oil quenching, subjected to cycles of one-sided three-point bending. The fatigue fractures were compared with the results of fatigue strength studies of 16MnCr5 steel following low-pressure carburizing and nitrogen quenching. The fatigue tests for 16MnCr5 steel were conducted as part of a high-cycle resonance test, with a pendular bending load. The study also involved an analysis of the effects on non-metallic inclusions in the structure on the mechanism of fatigue destruction. The inclusions were found to initiate fatigue cracks. In both cases, a similar method of a fatigue fissure initiation was observed, independent of the study method or specimen material.

Keywords: Fatigue strength, non-metallic inclusions, thermo-chemical treatment

1. Introduction

The majority of loads present in machines that working movements are cycling loads that vary in time. They generate oscillating stress, usually resulting in shortening the life time of machine parts. The process, cased material fatigue, is important in designing the "life cycle" of a product. Loads present in such systems are usually generated at stress levels lower than in stresses caused by a static strength test [1] and is a significant feature in fatigue loads.

Fatigue strength is rather unpredictable and is affected by gravity, duration of load and its nature, how parts are constructed, material of the part and its structure. It has also been noted that non-metallic inclusions or discontinuities in the structure also generate fatigue damage, which result in destruction of a structure [2].

It is therefore still a significant issue, dating back to the 14th century', when it had to be dealt with in designing firearms and evaluating damage done to them. The development of this area started in the 1940's and it has continued to this day.

Carburizing, and particularly its modern variations, i.e. low-pressure carburizing, is one of the methods of steel treatment which can greatly improve its fatigue strength.

The main advantages of low-pressure carburizing over conventional methods include the considerable improvement of fatigue strength. For example, elimination of internal oxidation prevents the formation of surface indentations, which can be the centres of fatigue. Other advantages of low-pressure carburizing which can affect the fatigue strength include the fact that a clean, metallic surface of the items under treatment is obtained immediately after the process [3-6]. This can result in elimination of grinding and polishing when greater dimension tolerance is also acceptable. Conventional carburizing must almost always be followed by grinding, and the process is known [7,8] to introduce tensile stress to the surface layer, which is likely to decrease the fatigue strength. Therefore, application of this modern thermochemical treatment can improve the fatigue strength of steel significantly, although obviously, it cannot eliminate this type of destruction. It is therefore justified to conduct a study to determine the mechanism of fatigue destruction of steel following low-pressure carburization.

2. Specimen material

A 15CrNi6 steel of the chemical composition shown in Table 1 and 16MnCr5 steel, of the chemical composition shown in Table 2 were used in the fatigue tests. In both cases, the chemical composition of the alloy was determined by fluorescence X-ray spectroscopy. The carbon concentration in the examined steels was analyzed by the absorption of IR radiation method after burning the sample in an oxygen atmosphere.

TABLE 1

Chemical composition of 15CrNi6 steel [wt.%]

C	Mn	Si	P	Cr	Ni	Cu
0,12	0,57	0,26	<0,035	1,4	1,5	<0,3

* LODZ UNIVERSITY OF TECHNOLOGY, INSTITUTE OF MATERIALS SCIENCE AND ENGINEERING, 1/15 STEFANOWSKIEGO STR., 90-924 LODZ, POLAND,

Corresponding author: sebastian.lipa@p.lodz.pl

Chemical composition of 16MnCr5 steel [wt.%]

C	Si	Mn	Cr	Ni	Mo	Al	Cu	P
0,18	0,37	1,21	0,98	0,19	0,03	0,03	0,16	0,02

3. Thermo-chemical treatment of the specimens

Specimens made of 15CrNi6 steel were subjected to low-pressure carburizing by FineCarb® [9] technology in an atmosphere consisting of acetylene, ethylene and hydrogen [10]. The process temperature was 930°C, the total time (18 min. carburizing boost – 208 min. diffusion) and segmentation (8 – segments) of the process were selected so as to achieve an effective carburizing layer of 0.6 mm (for the 0.4%C criterion). Quenching was performed with cooling down to 870°C and holding for 30 minutes. Quenching was performed in Burgdorf H222 oil, at a stabilised temperature of 50°C. Subsequently, the specimens were tempered once at 185°C for 2h.

Specimens made of 16MnCr5 steel were subjected to low-pressure carburizing (LPC) – by FineCarb® technology. Low-pressure carburizing was performed in a VPT-4022/24IQN universal low-pressure carburizing furnace with the HPGQ at the temperature of 920°C. The total time (18 min. carburizing boost – 214 min. diffusion) and segmentation (8 – segments) of the process were selected so as to achieve an effective depth of 0.6mm (for the 0.4% C criterion). The working atmosphere was a mixture of hydrocarbons: acetylene and ethylene (1:1) diluted with hydrogen. After carburizing, the specimen was cooled down to 860°C and nitrogen quenching was performed at a pressure of p = 1.2 MPa. Quenching was followed by low tempering at 180°C for 2h. Figure 1 shows the carbon profiles for both cases. The carbon concentration in surface layer was measured with a Leco GDS 850A optical spectrometer. Carbon was determined for a few times after removing thin layers one by one, using grinding.
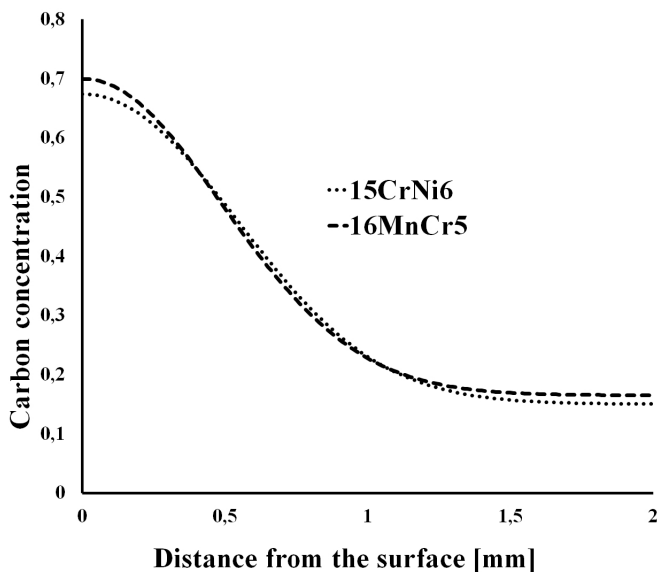

Fig. 1. The carbon profile diagram for both cases

4. A numerical analysis of the choice of a specimen shape for experimental studies

As part of the experiment for 15CrNi6 steel, a special specimen was designed, which was then subjected to a negative cyclic one-sided load in three-point bending [11,12]. The sample in Fig. 2a has a narrowing in the centre.
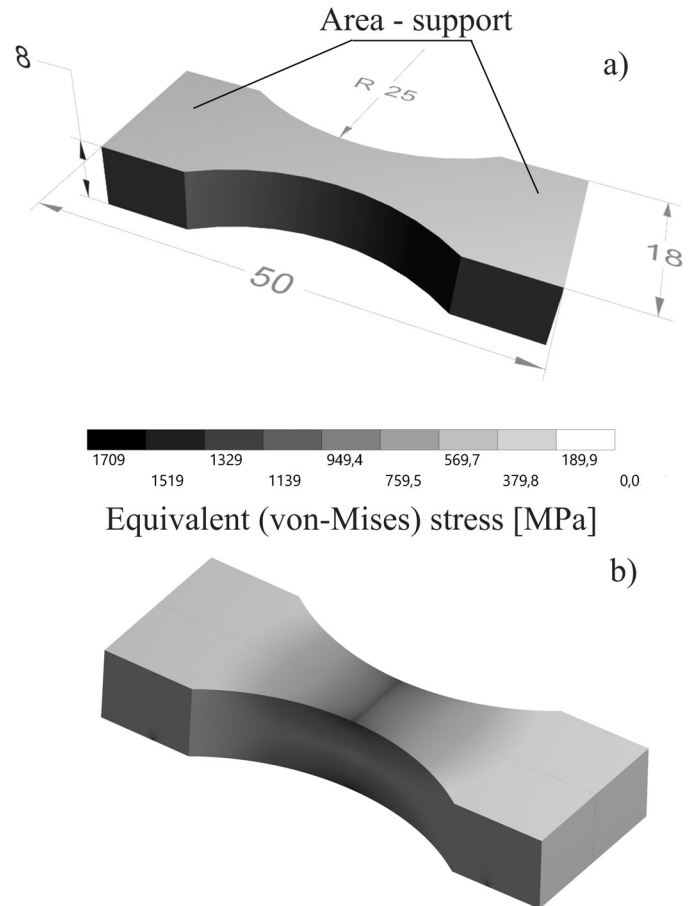

Fig. 2. a. The shape of the specimen designed for fatigue testing, b. distribution of von Mises reduced stress in a specimen for bending fatigue strength tests by the one-side three-point bending

This shape was necessary because of a decrease in the observation field of the fatigue fracture being formed. Given that it is common knowledge [13-15] that fatigue cracks in specimens subjected to thermochemical treatment are formed under the layer, thus making it invisible when initiated, the shape and load of the speciminspecimen therefore force the concentration of stress in one plane situated in the exact center. Additionally, it was proposed that the ends of the should be broadened, which reduces the unit load on the supports in the three-point bending. The specimen was subjected to a numerical analysis by the method of finite elements in order to verify the concept presented. The numerical computations were conducted in a Workbench Ansys 18.0 environment. The Cad model was divided into 8 body-type elements and MES discretization with Solid 186 elements was performed. All the body-type elements were connected with a "bonded" type contact with Conta 174

and Targe 170 elements. This produced a uniform specimen with 44544 hexagonal elements.

A specimen was supported on both sides with "supports displacement" and loaded at the centre with the force F.

The prepared model was subjected to numerical calculations. The map of stress in the specimen under study is shown in Fig. 2b. It confirms that the maximum stress is situated in the centre of the specimen, in the narrowed area. Before thermochemical treatment, the specimen was polished to eliminate any surface indentations.

A 16MnCr5 steel specimen was designed similarly. The guidelines of the ASTM E 606-04 standard [11], FEM simulations of distribution of deformations and stress and the experiments provided the base for developing the optimum shape and size for a specimen in terms of the possibility of achieving the desired deformations (stress) and conducting examinations of high-cycle bending fatigue strength by the resonance method (Fig. 3) [14,15].

Equivalent (von-Mises) stress [MPa]

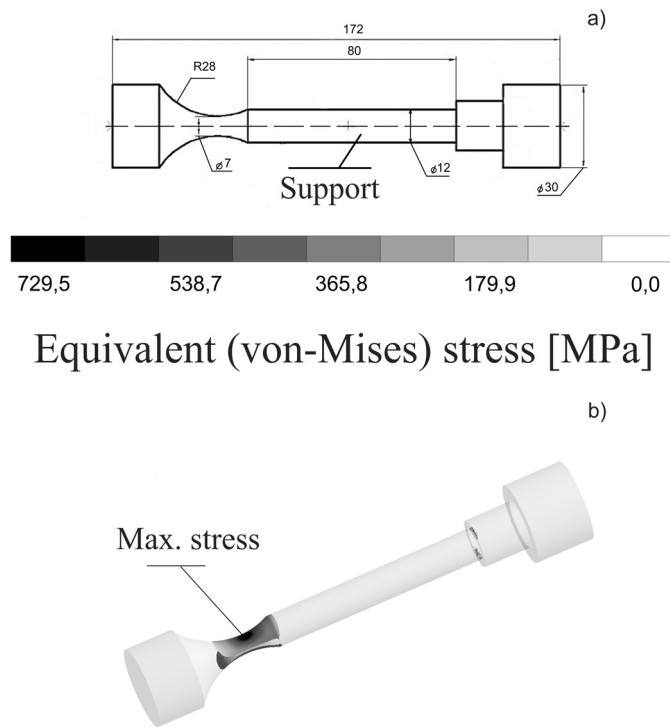| 729,5 | 538,7 | 365,8 | 179,9 | 0,0 |

Fig. 3. a) A specimen for bending fatigue strength tests by the resonance method [14,15], b) distribution of von Mises reduced stress in a specimen for bending fatigue strength tests by the resonance method [14,15]

5. Experiment methodology

A specimen made of 15CrNi6 steel (Fig. 2) was subjected to one-sided negative load in three-point bending at a test stand using a servo-hydraulic strength testing machine. The test was conducted on 16 specimens.

During the first stage, the specimen was loaded with the force of $P_m = -8$ kN in order to generate the mean stress of σ_m. This force lies within the elastic range of the specimen (Fig. 4). The P_m force is exactly half of P_{max}, which, when exceeded

even slightly [by ca. 10%], causes a permanent deformation of the structure. The idea behind the study methodology is that it is possible in extreme cases to subject a specimen to repeated one-direction stress, i.e. the average force P_m is equal to the variable cyclic force P_a corresponding to stress σ_a, which does not result in a change of the load sign.
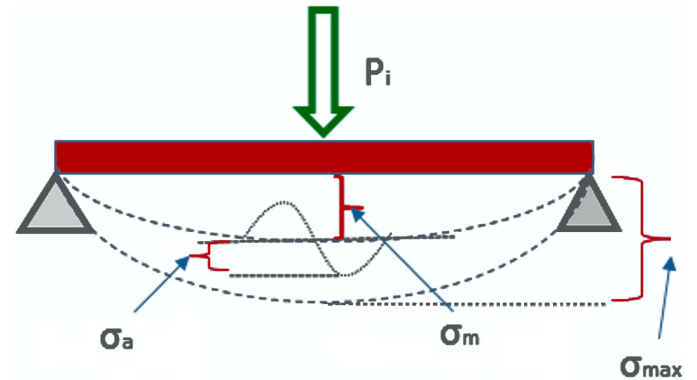

Fig. 4. Specimen load in a three-point bending test

Following this, the specimen was subjected to cyclic load while the force P_m remained unchanged; force P_a was selected so as to obtain characteristic points to plot the Wöhler curve.

Subsequently, the fatigue strength was determined by the resonance method for specimens made of 16MnCr5 steel [14,15] with a type TV50101/LS-80 TIRA inductor with a BAA1000 amplifier and a VR8500 measuring bridge, controlled by VibrationView software. The specimen deflection was determined with a laser extensometer fitted with an LTC 120-40 measuring head. The test was conducted on 16 specimens. The load for each sample was selected according to the step method based on specific elongation strength, and $0.7 \cdot R_m$ was taken as the initial load. Pendular bending of the specimens was conducted at the resonance frequency for each specimen, with the constant free end tilt amplitude. The stress was determined based on the deflection arrow. The moment when the fatigue crack occurred was detected as a change of the specimen's resonance frequency.

6. Experiment results

A Wöhler curve was plotted after the fatigue tests were conducted for limited and unlimited fatigue strength for both cases. The graphs are shown in Fig. 5. The fatigue strength of 15CrNi6 steel was determined to be $Zg = 1205$ MPa, whereas that of 16MnCr5 steel – $Zg = 670$ MPa (Fig. 5).

In the next stage, metallographic examinations of the fatigue fractures were conducted.

The examinations showed spheroid non-metallic inclusions under the carburized layer (Fig. 6). This form was not found in a fracture following quasi-static load for simple bending (Fig. 7).

Most likely, this form [a spheroid shape] results from cyclic three-directional impact of the matrix on an inclusion [16]. In
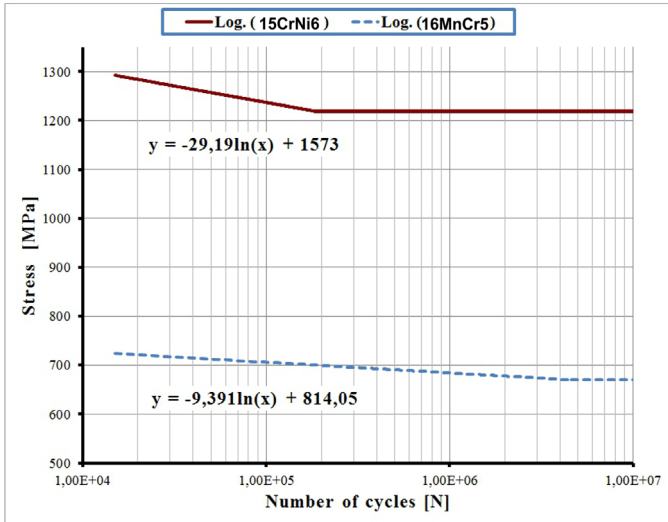
Fig. 5. Fatigue bending strength: 15CrNi6 and 16MnCr5 steel (Wöhler curve) following low-pressure carburizing in the FineCarb® technology
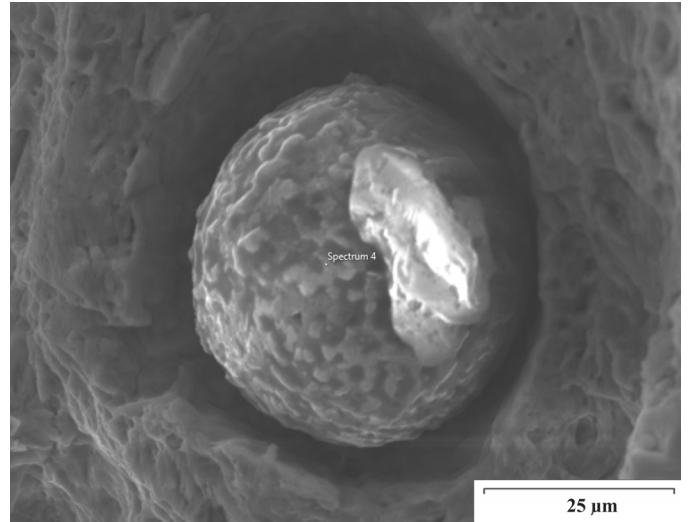

Fig. 6. A SEM image of a non-metallic inclusion revealed under a car-burized layer for 15CrNi6 steel following low pressure carburizing and oil quenching
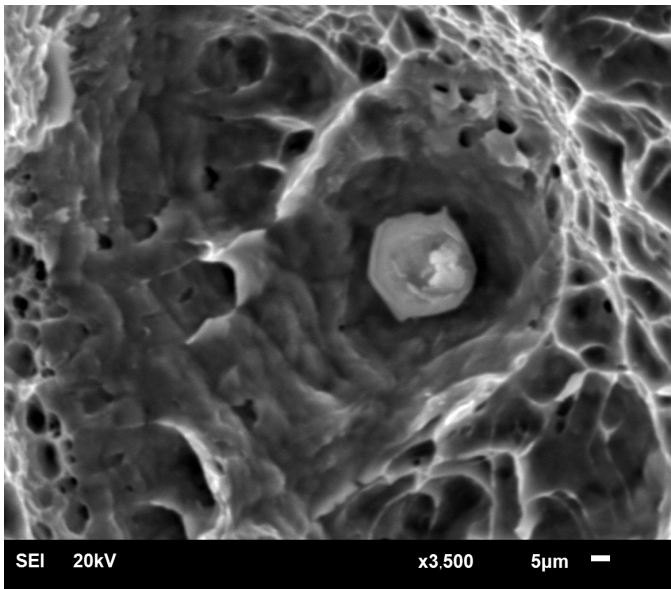

Fig. 7. A SEM image of non-metallic inclusions observed in quasi-static load in simple bending for 15CrNi6 steel following low pressure carburizing and oil quenching
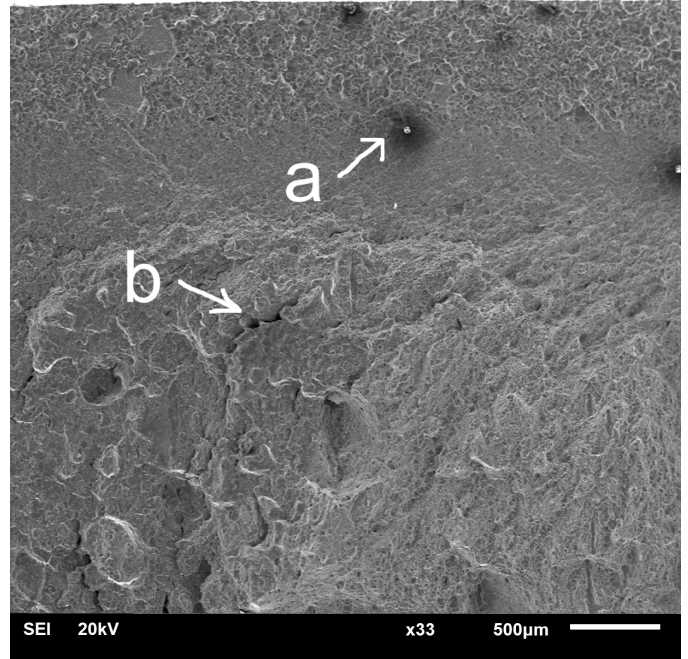

Fig. 8. A SEM image of a fatigue fracture for 15CrNi6 steel following low pressure carburizing and oil quenching; a. inclusion under the hardened surface with: a. formed "pocket", b. longitudinal cracks of the specimen

consequence of the variable load, a "pocket" is formed around an inclusion, followed by decohesion on the phase border, re-sulting in a crack [fissure]. This zone is highly plasticized. The SEM image (Fig. 8) of the whole fatigue fracture shows initiated fatigue fissures as well as sites where inclusions have weakened the material in the process of the fissure propagation, leading to local longitudinal "cracks" in the specimen.

A similar case was observed in a fatigue strength test of 16MnCr5 steel following carburization. Fractographic exami-nation of the fatigue fractures showed a fatigue centre directly under the carburized layer (Fig. 9).

The fatigue centre with beach marks propagating from it is spheroidal in shape (Fig. 10). A fatigue fissure also forms around the fatigue centre.

Chemical composition analyses were performed by EDX method at Oxford Analysis system equipped with X-MAX 80 EDS detector and appropriate software. Analyses were made from the area of depicted inclusions. Contamination phenom-enon, of course, deteriorates the analysis results for carbon and other element and was taken into considerations during studies. Software allows to take into account absorption caused by contaminated layer and its influence on the rest of element content results.

An in-depth analysis of the chemical composition spectrum of specimens made of 15CrNi6 steel (Fig. 11) has shown that the
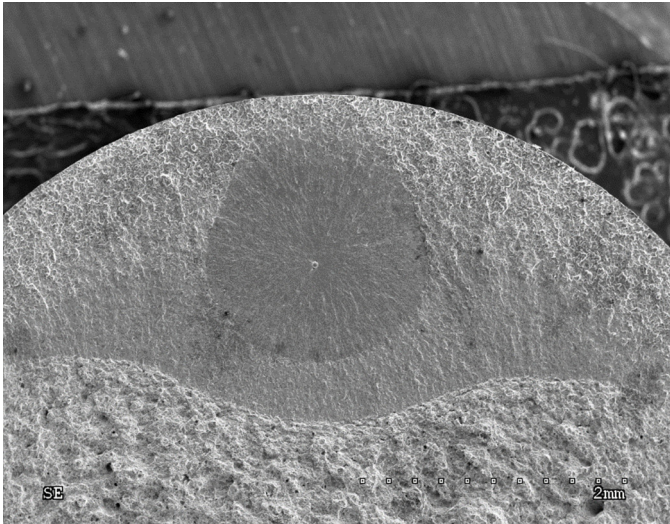
Fig. 9. A fatigue fracture of 16MnCr5 steel following low-pressure carburizing and nitrogen quenching, formed during the fatigue test conducted by the resonance method
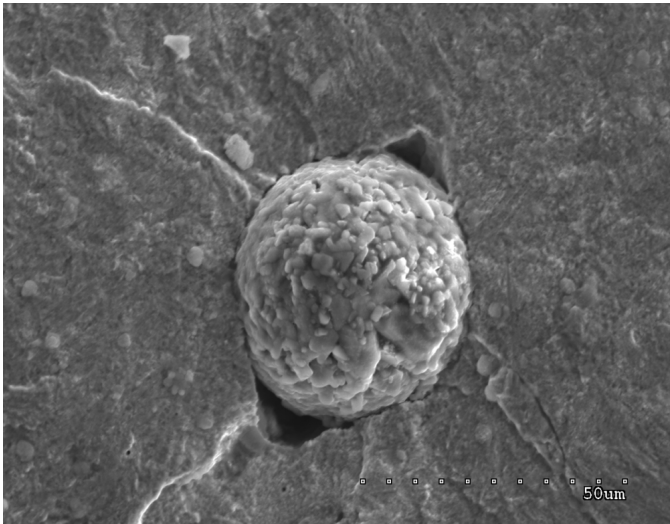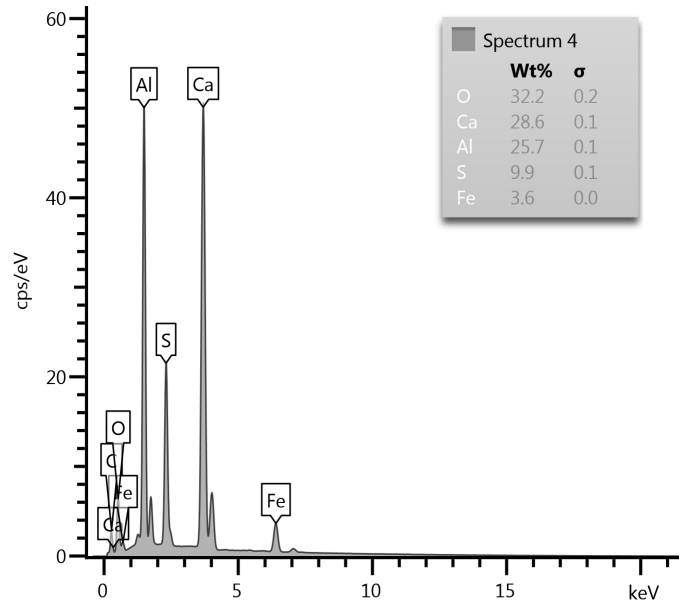

Fig. 11. X-ray microanalysis of a fatigue centre formed during a test conducted by the resonance method of a specimen of 15CrNi6 steel

Studies of the chemical composition of the spheroidite formed in 16MnCr5 steel have shown that such inclusions consist mainly of calcium and aluminum. This is similar to that in 15CrNi6 steel. The inclusions constitute nuclei of fatigue cracks under the layer hardened by carburization. This study has proved that these inclusions affect the mechanism of fatigue destruction of steel which is similar in both cases and does not depend on the fatigue test conducted or the steel type.

7. Conclusions

This fatigue test in a one-sided load cycle and a pendular cycle in two different test methods revealed the impact of non-metallic inclusions formed as a result of deoxidation of steel. The tests showed that the inclusions initiate fatigue processes under the hardened layer. Additionally, the mechanism of formation of a fatigue crack was also observed. The initiation of a fatigue fissure is linked to the formation of a "pocket" around an inclusion, which results in decohesion on a phase border. The observed effect of non-metallic inclusions on fatigue strength was also examined by Lemaitre and Zhou [2,18]. In their work they have shown that the observed non-metallic inclusions in the steel structure cause sudden loss of fatigue strength. These inclusions are crucial in the case of unlimited fatigue strength as well as high frequency which was proved in the work of Wang et al. [19]. In most cases the mechanism of fatigue destruction is influenced by the so-called fisheye formation. Hydrogen entrapped around non-metallic inclusions causes local decohesion at the boundary of two phases thus initiating a fatigue gap. A similar mechanism of initiation and propagation of a fatigue fissure has been observed in two different test methods – different types of steel and different loads in this paper.

Fig. 10. A fatigue centre of 16MnCr5 steel following low-pressure carburizing and nitrogen quenching, formed during the fatigue test conducted by the resonance method

non-metallic inclusions are composed of a compound of oxygen, aluminum and calcium, which can be identified as one formed as a result of deoxidation of steel with aluminum and calcium.

Products include two-component molecules of calcium aluminates $mCaO*nAl_2O_3$ and of anorthite and/or gehlenite: $CaO*Al_2O_3*2SiO_2$ and/or $2CaO*Al_2O_3*SiO_2$. The technology of deoxidation of steel with aluminum and calcium is well-known [17]. It is applied not only to reduce the amount of oxygen, but also to control and modify the physicochemical properties of non-metallic precipitates. It is usually applied in steel cast in the continuous technology to eliminate ingots congealing. Introducing calcium, whose solubility increases with the concentration of silicon and aluminum, helps to eliminate large inclusions and to modify the composition of other inclusions with a view to lowering their melting point.

1350

REFERENCE

[1] Z.L. Kowalewski, Directions and perspectives for the development of endurance research, ITS, Warsaw (2008).

[2] J. Lemaitre, A Course on Damage Mechanics, Springer, Berlin, Heidelberg (1996).

[3] W. Gräfen, B. Edenhofer, Surf. Coat. Technol. **200**, 1830-1836 (2005).

[4] P. Kula, R. Pietrasik, K. Dybowski, J. Mater. Process. Technol. **164-165**, 876-881 (2005).

[5] S. Preisser, F. Seemann, R. Zenker, Vacuum Carburizing with high pressure gas quenching – the application, 1st Int. Automotive Heat Treating Conf., 13-15 July, Puerto Vallarta, Mexico, 135-147 (1998).

[6] W. Stachurski, P. Zgórniak, J. Sawicki, M. Przybysz, Adv. Sci. Technol. Res. J. **11** (1), 237-245 (2017).

[7] Z. Gawroński, A. Malasiński, J. Sawicki, Int. J. Automot. Technol. **11** (1), 127-131 (2010).

[8] J. Sawicki, B. Kruszyński, R. Wójcik, Adv. Sci. Technol. Res. J. **11** (2), 17-22 (2017).

[9] Patent No.: EP 1558781, US 7,550,049 – Method for under-pressure carburizing of steel workpieces.

[10] Patent No.: EP 1558780, US 7,513,958 – Hydrocarbon gas mixture for the under-pressure carburizing of steel.

[11] ASTM Standards, E 606-04, Standard practice for strain-controlled fatigue testing, ASTM International (2005).

[12] PN-EN ISO 7438:2016-03, Metals – bending test (2016).

[13] P. Kula, K. Dybowski, S. Lipa, R. Pietrasik, R. Atraszkiewicz, L. Klimek, B. Janusewicz, E. Wołowiec , SSP. **225**, 45-52 (2015).

[14] K. Dybowski, P. Kula, S. Lipa, R. Pietrasik, Materials Engineering **31** (4), 939-941 (2010).

[15] K. Dybowski, P. Kula, R. Pietrasik, S. Lipa, Materials Engineering **32** (4), 392-394 (2011).

[16] M. Sozańska, Hydrogen destruction type „fish eyes" selected steel for energetics, Academic Press Silesian University of Technology, No.1705, Gliwice (2006).

[17] T. Lis, P. Różański, Metallurgist, Metallurgical News. **72** (5), 259-264 (2005).

[18] S. Zhou, Y. Murakami, S. Beretta, Y. Fukushima, Mater. Sci. Technol. **18**, 1535-1543 (2002).

[19] Q.Y. Wang, C. Bathias, N. Kawagoishi, Q. Chen, Int. J. Fatigue. **24**, 1269-1274 (2002).